



Electric field transition between the diffuse and streamer regions of sprites estimated from ISUAL/array photometer measurements

T. Adachi,¹ H. Fukunishi,¹ Y. Takahashi,¹ Y. Hiraki,¹ R.-R. Hsu,² H.-T. Su,² A. B. Chen,² S. B. Mende,³ H. U. Frey,³ and L. C. Lee⁴

Received 4 April 2006; revised 6 June 2006; accepted 12 June 2006; published 6 September 2006.

[1] We analyze optical data of twenty sprites and three halos observed by the array photometer which is a scientific instrument of the ISUAL payload on the FORMOSAT-2 satellite. The altitude distribution of electric field is derived from the ratio of blue to red emission intensity by assuming all emissions are due to the electron impact excitation of nitrogen molecules. We find a clear transition at ~ 75 km altitude from the upper-diffuse to lower-streamer region. Estimated electric field intensities in the diffuse region are $0.5\text{--}0.7 E_k$, which support the theoretical expectation that their optical emissions could be produced without significant ionization. On the other hand, those in the streamer region are $1\text{--}2 E_k$ which is a few times less than predicted fields in the streamer head. We suggest that this discrepancy is due to the long-lasting components such as the lower portions of the upward branches and bead structures. **Citation:** Adachi, T., H. Fukunishi, Y. Takahashi, Y. Hiraki, R.-R. Hsu, H.-T. Su, A. B. Chen, S. B. Mende, H. U. Frey, and L. C. Lee (2006), Electric field transition between the diffuse and streamer regions of sprites estimated from ISUAL/array photometer measurements, *Geophys. Res. Lett.*, 33, L17803, doi:10.1029/2006GL026495.

1. Introduction

[2] Recent imaging observations revealed spatio-temporal structures of sprites occurring at the mesospheric altitudes of 50–90 km in association with lightning discharges. *Gerken and Inan* [2002] carried out telescopic observations and clarified that sprites consist of fine structures with diameters of ~ 100 m which are considered to be streamers [*Liu and Pasko*, 2004]. *Stanley et al.* [1999] clarified development of columniform sprites and carrot sprites by 1-ms high-speed imaging observations. Columniform sprites consist of expanding columns and tendrils developing downward from their base. On the other hand, carrot sprites have additional branches developing upward from bright columns, leading to diffuse emissions often called “leaves” at their tops. Recently, *Cummer et al.* [2006] observed stationary bead structures left at the collision point of two tendril channels. Although it is clear that the bright components such as the lower portions of the upward branches and bead structures

have relatively long durations, no conclusive explanations for their persistence have been put forth until the present. *Pasko and Stenbaek-Nielsen* [2002] classified emission regions of sprites into two categories: the upper-diffuse region and the lower-streamer region. At altitudes of the diffuse region, a diffuse glow referred to as sprite halo is often observed to precede the occurrence of sprites. Theoretical studies have clarified that optical emissions of halos are recognized as manifestations of intense quasi-static electric fields induced by lightning discharges [*Barrington-Leigh et al.*, 2001].

[3] In addition to the imaging observation data, spectral data provide us essential information on the physical process of sprites since they enable us to estimate the intensities of electric fields inducing optical emissions [*Morrill et al.*, 2002; *Kuo et al.*, 2005; *Liu et al.*, 2006] (see section 4 of the present paper for details). *Morrill et al.* [2002] observed the streamer region of carrot sprites by a dual color CCD camera with a time resolution of ~ 17 ms. They estimated the electric fields in the upward branches and the tendrils as ~ 0.8 and $\sim 1.0 E_k$, respectively. Here, E_k of ~ 128 Td is the conventional dielectric breakdown field where $1 \text{ Td} = 10^{-17} \text{ V cm}^2$. *Kuo et al.* [2005] and *Liu et al.* [2006] estimated electric field intensities to be $2\text{--}4 E_k$ on the basis of the ISUAL/spectrophotometer measurements and pointed out that the estimated values reflect the electric fields in the head of individual streamers. Their observations without spatial resolution, however, provide us no information on the altitude dependence of electric fields. In summary, past observations are insufficient to investigate the spatial and temporal variations of electric fields inducing sprite emissions. In this study, we estimate electric field intensities of sprites from the ISUAL/array photometer data with high spatiotemporal resolution and discuss the physical processes causing sprite emissions by comparing the obtained results with past studies.

2. Instrumentation

[4] The Imager for Sprites and Upper Atmospheric Lightning (ISUAL) is a scientific payload on board the FORMOSAT-2 satellite, which was launched on May 20, 2004 [*Chern et al.*, 2003; *Kuo et al.*, 2005]. The FORMOSAT-2 has a sun-synchronous (9:30 to 21:30 local time) polar-orbit at an altitude of ~ 891 km with a period of 14 rev/day. The ISUAL consists of an image intensified CCD camera with a selectable six-color filter wheel, a six-color spectrophotometer (SP), and a dual-color array photometer (AP). Routine ISUAL measurements are carried out in the nighttime keeping its field-of-view (FOV) in the Earth’s limb direction.

¹Department of Geophysics, Tohoku University, Sendai, Japan.

²Department of Physics, National Cheng Kung University, Tainan, Taiwan.

³Space Sciences Laboratory, University of California, Berkeley, California, USA.

⁴National Applied Research Laboratories, Taipei, Taiwan.

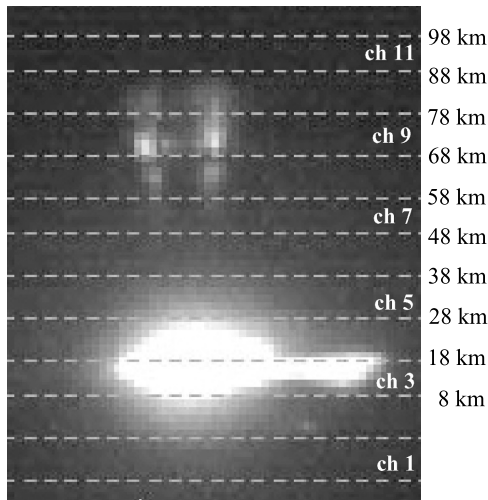


Figure 1. An image of sprites observed with ISUAL imager at 11:19:36 UT on September 13, 2004. White dotted lines demonstrate the fields of view of the array photometer.

[5] The image intensified CCD camera has a FOV of 20° (horizontal) \times 5° (vertical) and a filter turret with six filters (762, 557.7, 630, 427.8, 633–751 nm, and panchromatic). The exposure time is programmable within a range of 1–1000 ms. In this study, we use imager data obtained with the 633–751 nm filter and an exposure time of 15 or 30 ms. The SP consists of six photometers covering different wavelength ranges (150–280, 337, 391.4, 623–750, 777.4, and 250–390 nm), and has the same FOV as the CCD camera. The time resolution of SP is 100 μ s. Different from the CCD and SP, the AP provides us spectral information in a vertically narrow FOV by simultaneously measuring the two wavelength ranges of 360–470 and 520–750 nm selected by blue and red filters, respectively. Each photometer has vertically aligned 16 channels, and the FOV of each channel is 22.0° (horizontal) \times 0.23° (vertical) and the whole FOV is 22.0° (horizontal) \times 3.6° (vertical).

Thus, the vertical resolution of the AP is ~ 10 km for events occurring at 2500 km distance which enables us to detect emissions of sprites and lightning separately even if the delay time of sprites is significantly short (c.f., the SP analysis by Kuo *et al.* [2005]). The AP can detect fast temporal variation of sprites with a time resolution of 50 μ s for the initial 18 ms and of 500 μ s for the following 222 ms. The ISUAL data acquisition is performed for transient luminous events in which the output signal level of the SP exceeds an adjustable trigger criterion.

3. Observation and Data

[6] During the period from July 2004 to July 2005, the ISUAL has observed ~ 140 sprite events. Figure 1 shows an example of imager data observed at 11:19:36 (UT) on September 13, 2004. White dotted lines represent the FOV of individual channels of the AP. Sprites are seen in channels 7–10 while their parent lightning is seen in channels 3–4. Figure 2 represents concurrent array photometer data measured by channels 1 and 7–10, in which background emissions have been subtracted. Since channel 1 points below the causative lightning, temporal variation in this channel is due to scattering light from the lightning seen in channels 3–4. Consequently, double peak signals in channels 7–10 (solid lines) represent total emissions from lightning and sprites. Because of the coincidence of the first peaks in these channels with the peak in channel 1, they are concluded to be due to scattering light from the parent lightning. In order to derive pure sprite signals in the second peak, we scale the lightning signal level in channel 1 to the first peak in channels 7–10 (dotted lines) and subtract them from original data. Figure 3 represents the blue to red (B/R) ratios of derived sprite emissions (solid lines), in which we find a peak at the initial stage and subsequent exponential decay for each channel. The intensity of red emission, which is significantly weak initially, leads to large uncertainty in the B/R calculation. In order to derive reliable values of the initial peaks, we fit exponential curves (dotted lines) to the observed B/R ratios of the decaying periods by using the chi-square fitting method. In this event, the peak

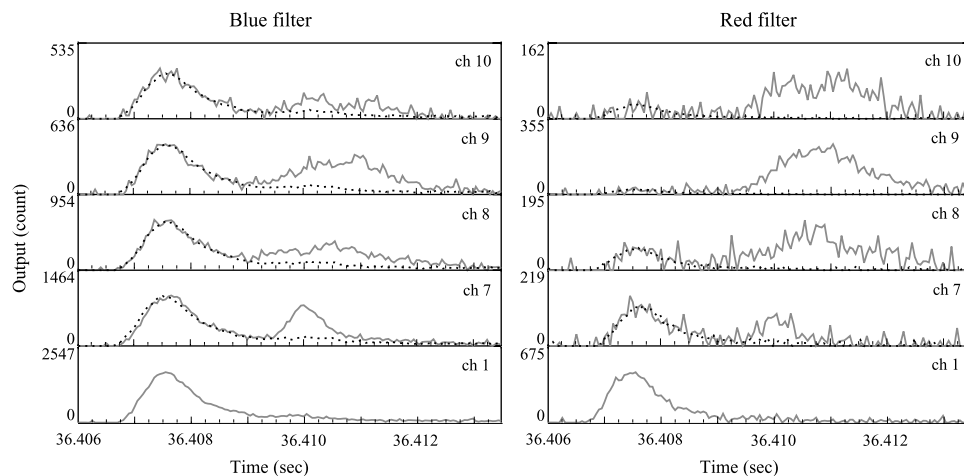


Figure 2. Temporal variations of (left) blue and (right) red emissions from sprite and parent lightning observed with the array photometer. Solid lines show original output signals while dotted lines represent temporal variations of channel 1 scaled to the first peak of each of channels 7–10.

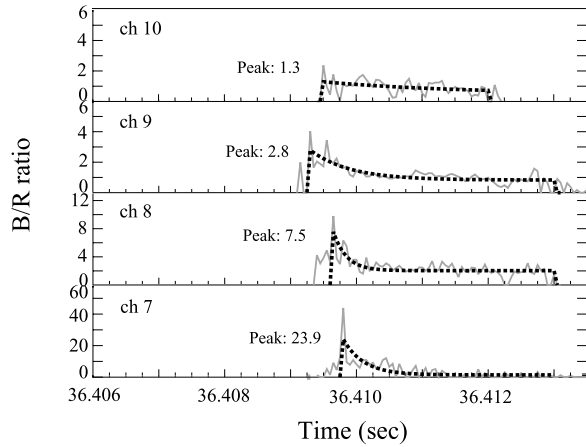


Figure 3. Temporal variations of observed blue/red (B/R) ratios of sprite emission (solid lines). Dotted lines represent exponential curve fitted to solid lines using the chi-square fitting method.

values of fitted curves in channels 7–10 are 23.9, 7.5, 2.8, and 1.3, respectively, which demonstrates that the B/R ratio becomes larger at lower altitude. In all the analyzed events, we find such tendencies that B/R ratios become large at the initial stage and at lower altitude.

4. Analysis

[7] From the B/R ratio, we estimate the electric field averaged in the FOV of each photometer channel and in time of 50 μ s. By assuming that electric field is uniform and quasi-steady, the production rate of optical emission through electron impact on air particles is written as $Ak(E/N)Nn_e$. Here, A is the Einstein coefficient, k is the excitation rate coefficient of a certain electronic state which is a function of electric field E reduced by the air density N , and n_e is the electron density. Since N and n_e are canceled out, the B/R ratio roughly is a function of E/N . We consider that the AP measures four band emission systems: N_2 second positive (2P) and N_2^+ first negative (1N) systems with blue filter, and N_2 first positive (1P) and N_2^+ Meinel (MN) systems with red filter. The B/R ratio is, then, expressed as follows.

$$\frac{B}{R} \text{ratio} = \frac{I(N_2 2P) + I(N_2^+ 1N)}{I(N_2 1P) + I(N_2^+ MN)} \quad (1)$$

The measured intensity I of each system summed up with lines of vibrational states (v' , v'') is written as

$$I = Nn_e \sum_{v'} \frac{k \cdot q_{v'} + f_{v'}}{1/\tau_{v'} + k_q[M]} \sum_{v''} A_{v'v''} T(\lambda_{v'v''}) S(\lambda_{v'v''}) \quad (2)$$

where $[M]$ is the density of species M ($= N_2$ or O_2), k_q is the quenching coefficient, and τ , q , f is the lifetime, the Franck-Condon factor, and the cascade effect of v' state, respectively. And T and S are the atmospheric transmittance and the absolute sensitivity of the AP, respectively, as functions of wavelength λ . Here, T is calculated with the MODTRAN-4 code. The values of τ , q , A , and λ are taken from *Gilmore et al.* [1992] where we assume for q that all

nitrogen molecules are in a ground state before electron impact. The value of k_q is from *Vallance Jones* [1974]. The electronic transition from C to B is considered as a cascade term f of $I(N_2 1P)$, otherwise $f = 0$. The value of k is calculated as a function of E/N by solving electron kinetics in air with a Monte Carlo method (Y. Hiraki and H. Fukunishi, Theoretical criteria of charge moment change by lightning for initiation of sprites, submitted to *Journal of Geophysical Research*, 2006). Because the loss term of excited state depends on $[M]$, the B/R ratio strictly is a function of altitude along with E/N . In order to estimate the altitude range covered by each photometer channel, we assume the upper limit of the sprite altitude to be 85 km and the altitude of the maximum intensity of lightning flash to be 15 km that is a typical altitude of thundercloud top at low latitudes. We note that $[M]$ is the most sensitive parameter causing large uncertainty in E/N and the resultant analytical errors are given quantitatively in the following section.

5. Results

[8] Figure 4 shows the modeled B/R ratios using equations (1) and (2) as well as the observed peak values for the event in Figures 1–3. Here, we consider the spatiotemporal development of sprites for the precise estimations of the emission altitudes. As shown in Figure 3, sprite emission starts at channel 9 with upward motion toward channel 10 and downward motion toward channel 7. Consequently, the initial peaks of the B/R ratios in channels 8 and 7 come from the upper edge of each FOV, whereas the initial peak in channel 10 comes from the lower edge of its FOV. As for channel 9, we assume the initial emission comes from the middle altitude of FOV. The E/N values for the initial peaks in channels 7–10 are thus estimated as 149 Td at 58 km, 129 Td at 68 km, 82 Td at 73 km, and 62 Td at 78 km, respectively.

[9] Similarly, we have analyzed 20 sprite events and 3 halo events in which AP data have sufficient signal-to-noise ratios ($>10\sigma$, where σ is the standard deviation) in both red and blue photometer channels. Estimated altitude profiles of the reduced electric field E/N are compared with the conventional air breakdown field ($E_k \sim 128$ Td) in Figure 5. Diamonds represent sprite events while asterisks represent halo events. We clearly find a transition of the reduced electric

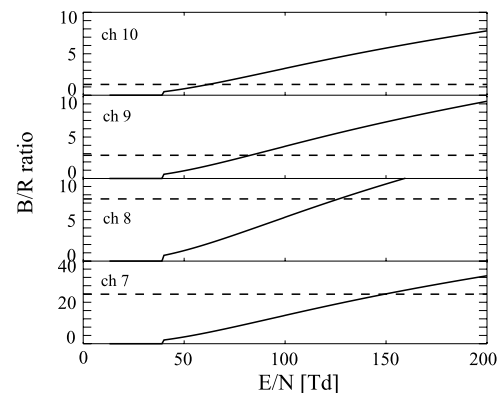


Figure 4. Modeled B/R ratio as a function of E/N (solid lines) as well as the peak B/R ratio (dotted lines) observed by the AP at channels 7–10.

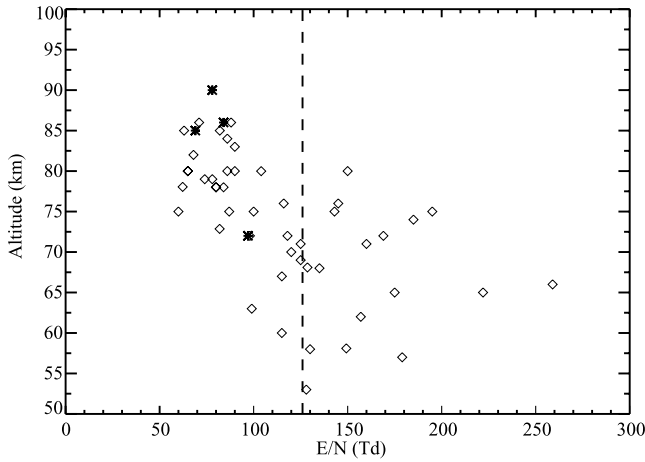


Figure 5. Altitude profiles of E/N of sprite events (diamonds) and halo events (asterisks) as well as the conventional air breakdown field $E_k \sim 128$ Td (dashed line).

field around 75 km. Electric field intensities above the transition are estimated to be 60–90 Td and 70–90 Td for sprite and halo events, respectively, while those below the transition are 100–260 Td.

[10] As seen in Figure 5, errors in the altitude estimation make larger variations in the electric fields at lower altitudes because the quenching term $k_q[M]$ of equation (2) increases exponentially as the altitude decreases. By considering variations of 10 km in the topside altitude of sprites, the estimation errors of electric field are calculated to be ± 4 Td at 80 km and ± 40 Td at 60 km. We note that uncertainties in the parameters except $[M]$ in the equation (2) cause errors of only $\sim 1\%$ in E/N , which could be neglected in this analysis.

6. Discussion

[11] We compare the altitude dependence of electric field intensity with the results reported by *Pasko and Stenbaek-Nielsen* [2002]. They analyzed 25 sprite events observed with a low-light level camera and found transitions between the upper-diffuse and the lower-streamer region at altitudes of 78.2 ± 4 km. Since their results are close to our transition altitudes of 75 ± 5 km, we suggest that the altitude variation of electric fields are associated with morphological transitions of sprites.

[12] As shown in Figure 5, we estimate reduced electric fields of 60–90 Td in the diffuse region of sprites and halos. We note that the conventional breakdown field E_k of ~ 128 Td is defined as electric field intensity at which the ionization rate coefficient is comparable to the attachment coefficient. The attachment process dominates at $E < E_k$ while ionization dominates at $E > E_k$. Therefore, ionization would be negligible in the diffuse region of sprites and halos since the estimated values are smaller than E_k . Even though significant ionization does not occur, it is theoretically possible that emissions of nitrogen molecules are still observable at 60–90 Td, because the ratio of the excitation rate coefficient at 80 Td to those at $E_k \sim 128$ Td is no less than 0.4 at the N_2 $B^3\Pi_g$ state (the upper electronic state of N_2 1P band) and no less than 0.1 at the N_2 $C^3\Pi_u$ state (those of N_2 2P band). Here, we have to note that the

number of halo events analyzed in the present study would not be statistically sufficient. We emphasize, however, that these halo events certainly have smaller electric field intensities than E_k , because the estimation error is only ± 4 Td.

[13] In contrast, we estimate reduced electric fields of 100–260 Td in the streamer region of sprites. Thus, significant ionization would occur in this region since the estimated electric field intensities are larger than E_k . *Morrill et al.* [2002] observed sprites with a dual-color CCD camera and estimated electric field intensities which is significantly smaller than E_k at altitudes of 55–65 km. Since the temporal resolution of their imaging observation is ~ 17 ms, in contrast to 50 μ s of the AP, the electric field intensities are interpreted as temporally averaged values. *Kuo et al.* [2005] analyzed ISUAL/spectrophotometer (SP) data and estimated electric field intensities to be two times larger than our estimation. Note that their analysis is based on the emission intensity of the N_2^+1N and N_22P band systems while we analyzed data from the AP that primarily observes the N_21P and N_22P band systems. We see in Figure 4 of *Kuo et al.* [2005] that the maximum intensity of N_2^+1N (SP3) emissions precedes the maximum intensities of N_22P (SP2) and N_21P (SP4) emissions. Therefore, it is likely that results by *Kuo et al.* [2005] correspond to the initial stage of streamer development where the N_2^+1N and N_22P emissions are sufficiently bright, while our results correspond to the following stage where the N_21P and N_22P emissions are sufficiently bright.

[14] *Liu et al.* [2006] recently compared the results obtained from a modeling study with the ISUAL/SP measurements. They found that the streamer modeling agrees well with the ISUAL measurements during the initial ~ 0.5 ms but may not be applicable at the following stage. Similarly, our results show that electric field intensities are two or three times smaller than the theoretical prediction of sprite streamer by *Liu and Pasko* [2004], which implies that the streamer modeling fails in explaining the experimental data at the later stage. *Cummer et al.* [2006] observed sprite development with a high-speed CCD camera. They reported that streamers initially propagate downward, branch into multiple channels, and fade with half-life of ~ 0.8 ms. We note that this decay time is close to the time constant (~ 0.5 ms) of the initial stage of streamer development during which streamer modeling would be applicable [*Liu et al.*, 2006]. At the following stage, a bright column expands upward and downward accompanying with multiple bead structures below them, and subsequently streamers develop upward from the bright column, resulting in the brightest stage of sprites [*Cummer et al.*, 2006]. As mentioned above, our results probably correspond to this brightest stage and show two or three times smaller electric fields than the theoretical predictions of sprite streamers. Since the optical emission intensity is generally expressed as $Ak(E/N)Nn_e$ where A and N are almost constant, electron density n_e would be sufficiently large at this brightest stage where E/N is relatively small.

7. Conclusions

[15] The ISUAL/array photometer provides us spatiotemporal structures of sprites by simultaneously measuring blue and red emissions. The blue/red (B/R) emission ratios have

the maximum value initially and exponentially decrease with time. The altitude distribution of reduced electric field is derived from the peak B/R ratio. We find a clear transition of the electric fields at altitude of ~ 75 km, which correspond to their morphological transition. The magnitudes of electric fields in the diffuse regions of sprites and halos are 60–90 Td with possible errors of ~ 4 Td, supporting theoretical expectations that diffuse emissions could be produced without significant ionization process. On the other hand, those in the streamer region of sprites are 100–260 Td with possible errors of ~ 40 Td which is a few times smaller than the predicted fields in the head of single streamer. This discrepancy would be due to the bright and persistent components such as the lower portion of the upward branches and bead structures in sprites.

[16] **Acknowledgments.** This work is supported by research grant, 93-NSPO(B)-ISUAL-FA09-01. TA is supported by a grant of Research Fellowships of the Japan Society for the Promotion of Science for Young Scientists.

References

- Barrington-Leigh, C. P., U. S. Inan, and M. Stanley (2001), Identification of sprites and elves with intensified video and broadband array photometer, *J. Geophys. Res.*, *106*, 1741–1750.
- Chern, J. L., R.-R. Hsu, H.-T. Su, S. B. Mende, H. Fukunishi, Y. Takahashi, and L. C. Lee (2003), Global survey of upper atmospheric transient luminous events on the ROCSAT-2 satellite, *J. Atmos. Sol. Terr. Phys.*, *65*, 647–659.
- Cummer, S. A., N. Jaugey, J. Li, W. A. Lyons, T. E. Nelson, and E. A. Gerken (2006), Submillisecond imaging of sprite development and structure, *Geophys. Res. Lett.*, *33*, L04104, doi:10.1029/2005GL024969.
- Gerken, E. A., and U. S. Inan (2002), A survey of streamer and diffuse glow dynamics observed in sprites using telescopic imagery, *J. Geophys. Res.*, *107*(11), 1344, doi:10.1029/2002JA009248.
- Gilmore, F. R., R. R. Laher, and P. J. Espy (1992), Franck-Condon factors, r-centroids, electronic-transition moments, and Einstein coefficients for many nitrogen and oxygen band systems, *J. Phys. Chem. Ref. Data*, *21*, 1005–1107.
- Kuo, C. L., R. R. Hsu, H. T. Su, A. B. Chen, L. C. Lee, S. B. Mende, H. U. Frey, H. Fukunishi, and Y. Takahashi (2005), Electric fields and electron energies inferred from the ISUAL recorded sprites, *Geophys. Res. Lett.*, *32*, L19103, doi:10.1029/2005GL023389.
- Liu, N., and V. P. Pasko (2004), Effects of photoionization on propagation and branching of positive and negative streamers in sprites, *J. Geophys. Res.*, *109*, A04301, doi:10.1029/2003JA010064.
- Liu, N., et al. (2006), Comparison of results from sprite streamer modeling with spectrophotometric measurements by ISUAL instrument on FORMOSAT-2 satellite, *Geophys. Res. Lett.*, *33*, L01101, doi:10.1029/2005GL024243.
- Morrill, J., et al. (2002), Electron energy and electric field estimates in sprites derived from ionized and neutral N₂ emissions, *Geophys. Res. Lett.*, *29*(10), 1462, doi:10.1029/2001GL014018.
- Pasko, V. P., and H. C. Stenbaek-Nielsen (2002), Diffuse and streamer regions of sprites, *Geophys. Res. Lett.*, *29*(10), 1440, doi:10.1029/2001GL014241.
- Stanley, M., P. Krehbiel, M. Brook, C. Moore, W. Rison, and B. Abrahams (1999), High speed video of initial sprite development, *Geophys. Res. Lett.*, *26*, 3201–3204.
- Vallance Jones, A. V. (1974), *Aurora*, Springer, New York.
- T. Adachi, H. Fukunishi, Y. Hiraki, and Y. Takahashi, Department of Geophysics, Tohoku University, Sendai, 980-8578, Japan. (adachi@pat.geophys.tohoku.ac.jp; fuku@pat.geophys.tohoku.ac.jp; hira@pat.geophys.tohoku.ac.jp; yukihiro@pat.geophys.tohoku.ac.jp)
- A. B. Chen, H.-T. Su, and R.-R. Hsu, Department of Physics, National Cheng Kung University, Tainan, 70101, Taiwan. (alfred@phys.ncku.edu.tw; htsu@phys.ncku.edu.tw; rrhsu@phys.ncku.edu.tw)
- H. U. Frey and S. B. Mende, Space Sciences Laboratory, University of California, Berkeley, CA 94720-7450, USA. (hfrey@ssl.berkeley.edu; mende@ssl.berkeley.edu)
- L. C. Lee, National Applied Research Laboratories, Taipei 106, Taiwan. (loulee@narl.org.tw)